Published in final edited form as:
Dev Biol. 2010 May 15; 341(2): 360–374. doi:10.1016/j.ydbio.2010.02.029.

Regulation of cell shape, wing hair initiation and the actin cytoskeleton by Trc/Fry and Wts/Mats complexes

Xiaolan Fang and **Paul N. Adler**
Department of Biology, Department of Cell Biology, Morphogenesis and Regenerative Medicine Institute and Cancer Center, University of Virginia, Charlottesville, VA 22903, USA

Abstract

The two NDR kinase family genes in *Drosophila* are *tricornered* (*trc*) and *warts* (*wts*). Previous studies on *trc* have focused on its role in the morphogenesis of extensions of epidermal cells and in dendrite branching and tiling. Studies on *wts* have focused on its roles as a tumor suppressor, in controlling photoreceptor type and in the maintenance of dendrites. Here we examine and compare the function of these genes in wing cells prior to their terminal differentiation. Mutations in these genes lead to changes in cell shape, cellular levels of F-actin, the timing of differentiation, and the expression of *multiple wing hairs* and DE-Cadherin. We showed that the effects of *wts* on all of these processes appear to be mediated by its regulation of the Yorkie transcription factor. We also provide evidence that *trc* regulates the expression of *DE-cadherin* and *mwh.* In addition, we showed that the effects on cell shape and the timing of differentiation appear to not be linked to changes in relative growth rate of cells compared to their neighbors.

Keywords

NDR; *trc*; *fry*; *wts*; *mats*; *yorkie*; Mwh; DE-Cadherin; cell shape; wing hair differentiation

Introduction

In animals there are two subfamilies of NDR kinases. In *Drosophila* these are encoded by the *tricornered (trc)* and *warts (wts,* also known as *lats-large tumor suppressor)* genes. These genes are thought to have largely separate functions but several intriguing connections have been uncovered. Mutations in *trc* lead to alterations in sensory neuron dendrite tiling and branching, to epidermal cells forming multiplied and branched hairs and arista laterals and to branched and deformed sensory bristles (Emoto et al., 2004; Geng et al., 2000). In these cell types Trc function is dependent on the presence of the large Fry protein and a member of the Mob (Mps One Binder) family (Cong et al., 2001; Emoto et al., 2004; He et al., 2005a; He et al., 2005b; Luca and Winey, 1998). These functions are conserved in organisms from yeast to flies (Bidlingmaier et al., 2001; Colman-Lerner et al., 2001; Du and Novick, 2002; Emoto et al., 2004; Nelson et al., 2003; Racki et al., 2000; Verde et al., 1998; Waldemar J. Racki, 2000; Weiss et al., 2002; Zallen et al., 2000). For example, the Trc and Fry homologs in *Caenorhabditis elegans*, Sax-1 and Sax-2, regulate mechanosensory dendrite tiling by

Correspondence to P. N. Adler, Department of Biology, University of Virginia, Charlottesville, VA 22903, USA. pna@virginia.edu. Tel: +1 (434) 982-5475.

controlling the termination point of sensory dendrites (Gallegos and Bargmann, 2004; Zallen et al., 2000). In *Saccharomyces cerevisiae*, mutations in CBK1 (*trc* homolog), TAO3 (*fry* homolog) and MOB2 impair the polarized growth of buds and later lead to a failure of daughter-cell specific transcription. In mammals there are two Trc-like NDR kinases. These have not yet been shown to regulate polarized growth, but interestingly NDR1 has been shown to be important in centriole duplication (Hergovich et al., 2007) and in spindle function in cell division (Chiba et al., 2009). The downstream targets of Trc-like NDR kinases that regulate polarized growth and the levels at which they act remain unclear.

The Wts kinase also requires a Mob family protein partner for its function, which in *Drosophila* is the Mats protein (He et al., 2005a; Lai et al., 2005). Wts kinase and Mats are part of the Hippo pathway that regulates cell proliferation (Emoto et al., 2006; Justice et al., 1995; Wei et al., 2007). In *Drosophila melanogaster*, Wts is downstream of and activated by phosphorylation by the Hippo (Hpo) kinase (Emoto et al., 2006). In both mammals and flies these genes act as tumor suppressors and loss of function mutations lead to tissue overgrowth. In addition, *wts* mutations lead to a failure of sensory neurons to maintain the normal pattern of dendritic branching and a failure in the specification of R8 photoreceptor subtypes (Mikeladze-Dvali et al., 2005). Wts is believed to function by phosphorylating Yorkie (Yki), leading to its translocation from the nucleus to the cytoplasm (Dong et al., 2007). In the nucleus Yki associates with Scalloped (SD) and functions as a co-activator (Wu et al., 2008; Zhang et al., 2008). Active Yki leads to increased expression of *cyclin E* and the anti-apoptosis gene *DIAP1* (*Drosophila inhibitor of apoptosis 1*) and such changes in gene expression are thought to be responsible for the overgrowth of clones of *hpo*, *wts* or *mats* loss of function mutations and to the overgrowth of clones that over express Yki (Wu et al., 2008; Zhang et al., 2008). Interestingly, Yki also promotes the expression of *expanded* (*ex*), which functions upstream of and activates the Hpo pathway (Hamaratoglu et al., 2006; Wu et al., 2008). Hence there is a negative feedback built into the system that functions to maintain constant pathway activity.

Although there are clear differences between the Trc and Wts pathways, they are also connected in several ways. One connection is that Hpo acts upstream of both Wts and Trc in da neurons. The role of Hpo in activating Wts is better known but it has also been established that Hpo can phosphorylate and activate Trc and genetic experiments demonstrated this was functionally important in da sensory neurons (Emoto et al., 2006). A second connection is that both *trc* and *wts* mutant cells have elevated levels of F-actin (He et al., 2005a). However, we previously noted that there were several phenotypes of *trc* or *fry* mutant cells in the wing epithelial that were the inverse of the phenotypes of *wts* or *mats* cells (He et al., 2005a; He et al., 2005b). For example, *trc* or *fry* mutant cells had an increased cross sectional area while *wts* or *mats* mutant cells had a decreased cross sectional area. In this paper we expanded on those findings and found that *hpo* loss of function clones and *yki* over expression clones shared this *wts* and *mats* mutant phenotype in wing epithelial cells. That *yki* over expression mimicked the *wts* phenotype implied that changes in gene expression were responsible for the changes in cell shape. We further extended these observations by obtaining and analyzing optical stacks of images of mutant clones. We found that the height of *wts* and *mats* mutant cells was increased and this compensated for the decreased cross sectional area so that there was no significant change in cell volume compared to wild type. In contrast, *trc* and *fry* mutant cells did not have altered cell height and thus that they showed an increase in cell volume.

How cell dimensions are controlled is poorly understood. One suggestion is that the height of epithelial cells is modulated by the balance between intercellular adhesion versus cell-matrix adhesion (Montell, 2008). Cadherins are central to intercellular adhesion. As a test of whether or not the increased cell height found in *wts* and *mats* clones was associated with increased intercellular adhesion, we examined DE-Cadherin levels in mutant clones. As might be predicted by the adhesion balance model we found increased levels of DE-Cadherin in *wts* or

mats mutant cells. However, we also observed increased DE-Cadherin in *trc* and *fry* mutant cells whose cell height was unchanged. Further, we did not see an increase in cell height in cells where *ptc-Gal4* was used to drive higher than normal levels of DE-Cadherin. Our data suggested that alterations in DE-Cadherin levels were insufficient to explain changes in cell height. Increased DE-Cadherin levels could be due to many different mechanisms. We found that mutations in both *wts* and *trc* lead to increased expression of B-galactosidase from an enhancer trap insertion into the *shotgun* (*shg*) gene (*shg* encodes DE-Cadherin in flies) establishing that at least in part the increase in DE-Cadherin is mediated at the transcriptional level.

Hair morphogenesis is part of the terminal differentiation program for wing epidermal cells. We previously found that *trc* (and *fry*) and *wts* (and *mats*) mutations resulted in opposite phenotypes on the timing of hair initiation. *trc* and *fry* mutant cells are delayed in hair initiation while *wts* and *mats* mutant cells differentiate precociously (He et al., 2005a). Thus, in this context one wild type function of *wts* appears to be to inhibit the terminal differentiation of wing cells. This is unusual for a tumor suppressor gene. We extended our previous results and found that loss of *hippo* function and *yki* over expression also shared the precocious differentiation phenotype of *wts* and *mats* mutant cells. Interestingly, *yki* loss of function clones showed delayed hair initiation and *yki* was epistatic to *wts*. The expression of the *mwh* gene increases around the time of hair initiation and this is a functionally important part of the hair morphogenesis program (Yan et al., 2008). We found that *yki* over expression could lead to increased *mwh* expression, but this was seen only around the time of hair morphogenesis, suggesting that *yki* over expression led to the premature initiation of the hair gene expression program. We also found that loss of *trc* and *fry* function led to decreased *mwh* expression at the time of hair initiation. This was consistent with the hypothesis that the mutations resulted in a delay in the hair gene expression program. The decreased *mwh* expression in *trc* cells was insufficient to explain their strong multiple hair phenotype as genetic experiments showed these genes functioned in parallel to control hair number.

Materials and Methods

Fly stocks and crosses

To induce *wts* or *mats* somatic clones we crossed *w hs-flp; FRT82 wts^{P3}/TM6 or w hs-flp; FRT82 mats^{e03077}/TM6* flies with *w hs-flp; FRT82 Ubi-GFP/FRT82 Ubi-GFP* flies. The larvae were heat shocked on the 3rd day after egg-laying.

To induce *trc* or *fry* clones, we crossed *w hs-flp; FRT80 trc^{p}/TM6* or *w hs-flp; FRT80 fry^{T2K61}/TM6* with *w hs-flp vg-Gal4; FRT80 Ubi-GFP/FRT80 Ubi-GFP* flies.

To induce *MINUTE* clones, we crossed *w hs-flp; FRT82 RpS17^{4} Ubi-GFP/TM6* with *w hs-flp; FRT82/FRT82*. The larvae were heat shocked on the 5th day after egg-laying to induce clones.

To induce *trc-wts* double mutant cells, we crossed *w hs-flp; ptc-Gal4 UAS-MCD8-GFP; FRT 82 wts^{P3}/TM6* with *w hs-flp; UAS-trc$^{S292A\ T453A}$; FRT82 tub-gal80ts* flies and heat-shocked the larvae on the 3rd day after egg-laying to induce clones and then shifted the pupae to 29°C to inactivate the temperature sensitive Gal80 protein and to activate Gal4 driven expression of the dominant negative Trc protein.

To induce *hippo* clones, we crossed *w hs-flp; FRT42Ubi-GFP* with *FRT42D hippo42^{47}/CyO* and heat shocked the larvae on the 3rd day after egg-laying.

To induce *yorkie* clones, we crossed *w hs-flp; FRT42D Ubi-GFP* with *FRT42D yki^{B5}/CyO* and heat shocked the larvae on the 2nd day after egg-laying. To induce cells that over-expressed

wild type Yorkie, we crossed *w hs-flp; Ay-Gal4 UAS-GFP* with *UAS-Yki/TM6*. Larvae were heat shocked for half an hour on the 4th day after egg-laying or for one hour on the 5th day after egg-laying.

To induce *wts yki* double mutant clones we crossed *w hs-flp; yki*^{B5}*/CyO; FRT82 wts*^{P3}*/TM6* females and *w hs-flp; yki*^{B5}*/Gla; FRT82 ubi-GFP P{tub-yki}/TM6* males. The *P{tub-yki}* transgene is a full-length *yki* cDNA driven by the ubiquitous α-tubulin promoter and this provides rescue of the mutation in the endogenous gene (Huang et al., 2005). The Gla chromosome contained the Bc marker, which allowed us to exclude that genotype. Flies that carried the CyO chromosome contained a wild type *yki* gene and they produced typical *wts* "tumor clones". The larvae were heat shocked on the 3rd day after egg-laying.

To induce *mwh* clones, we crossed *w hs-flp; FRT80 mwh* with *vg-Gal4 UAS-FLP; FRT80 Ubi-GFP*. To induce *ultA* mutant clones, we crossed *w hs-flp; FRT40 ultA/CyO*, with *w hs-flp; FRT40 Ubi-GFP* flies. The larvae were heat shocked on the 3rd day after egg-laying.

To induce cells that over-expressed wild type DE-Cadherin, we crossed *UAS-DE-Cadherin* with *ptc-Gal4* (this resulted in flies that expressed DE-Cadherin in the *patched* domain) or *Ay-Gal4 UAS-GFP* flies (which then induced GFP marked flip-out clones). For the cross involving *Ay-Gal4* the larvae were heat shocked for half an hour on the 4th day after egg-laying or for one hour on the 5th day after egg-laying.

To induce *mwh trc* or *mwh fry* double mutant clones, we crossed w *hs-flp; FRT80 mwh*^{1} *trc*^{1}*/TM6C,* or *w hs-flp; FRT80 mwh*^{1} *fry*^{1}*/TM6* with *UAS-flp vg-Gal4; FRT80 Ubi-GFP* flies. The larvae were heat shocked on the 3rd day after egg-laying.

FRT42 hpo^{42}*/CyO, FRT42 yki*^{B5}*/CyO* and *UAS-Yki/TM3* flies were generously provided by the Pan Lab at John Hopkins University. *th*^{j5c8} *(diap1-lacZ)/[TM3, Sb], CycE[16.4kb]-lacZ/ cycE[16.4kb]-lacZ* and *FRT40A ex*^{e1}*/CyO* flies were generously provided by Halder lab at University of Texas, M.D. Anderson Cancer Center. *y1 w67c23; P {lacW} shg*$^{k0340\ 1}$*/CyO* stock (#10377) and flies with *Ubi-GFP* and *FRT* containing chromosomes were obtained from the Bloomington Stock Center. Other mutation or transgenes containing stocks were either isolated in our lab and described previously (He et al., 2005a). The *fry* dsRNA fly stock (#40309) is from the Vienna *Drosophila* RNAi Center (VDRC).

In the experiments reported in this paper we chose to focus on single phenotypic null alleles. However, for *trc, fry, wts* and *mats* we have seen equivalent phenotypes with multiple alleles. Similar observations were also made in experiments where we used a transgene to induce RNAi for *trc* and *fry*.

Immunohistochemistry

Phalloidin-staining—White pre-pupae were collected and aged for the desired time and then pupae were pulled out from the pupal cuticle and fixed in 4% paraformaldehyde overnight. Pupal wings were cut off the body and pulled out from the wing cuticle. After being incubated in 1:200 Phalloidin/0.3%PBST (Phosphate Buffered Saline with Triton-100) solution for 2~3 hours, the wing was washed with 0.3%PBST solution three times (10 minutes each), and then rinsed in PBS solution, and finally mounted in ProLong Gold fluorescence mounting medium (Molecular Probes). Samples were then observed under confocal-fluorescent microscopy.

Immunostaining—White pre-pupae were collected and aged for the desired time, and then pupae were pulled out from the pupal cuticle and fixed in 4% paraformaldehyde for 2~3 hours. Pupal wings were cut off the body and pulled out from the wing cuticle. After being incubated in appropriate dilutions of primary antibody (varies with different antibodies) in 0.3%PBST

(PBS plus 0.3% triton X100) solution over night, the wings were washed with 0.3%PBST solution three times (15 minutes each), and then incubated in 1:200 secondary antibody/0.3% PBST solution for 2~3 hours. Then the wings were washed with 0.3%PBST solution three times (10 minutes each), then rinsed in PBS solution, and finally mounted in ProLong Gold fluorescence mounting medium. Samples were then observed under confocal fluorescent microscopy.

Antibodies

Anti-C-Fry antibody was raised in rabbits against a C-terminal peptide of Fry (He et al., 2005b). Anti-Mwh antibody was raised against a partial Mwh-GST fusion protein in rat at Spring Valley Laboratories, Inc. This antibody has been described previously (Yan et al., 2008). Anti-Trc antibody was raised in Rats at Spring Valley Laboratories, Inc. using purified Trc-GST protein (He et al., 2005b). Rabbit anti-GFP, Alexa phalloidin 488 and 568, anti-rabbit-488, anti-mouse 568 and anti-rat-568 antibodies were obtained from Invitrogen. Mouse anti-DE-Cadherin was obtained from Developmental Studies Hybridoma Bank (DSHB) at University of Iowa. Rabbit-anti-lacZ was obtained from ICN Biomedicals, Inc.

Scoring of Adult Wings

Wings were mounted in Euparal (Asco Labs, Manchester, England) and examined under bright-field microscopy.

Microscopy and Photography

A Spot digital camera (National Diagnostics, Manville, NJ) on a Zeiss Axioskop microscope (Thornwood, NY) was used to obtain the bright field images. For most experiments the samples were examined using an Atto spinning disc confocal attachment on a Nikon microscope. The MetaMorph software (Molecular Device, MDS Inc.) was used to take the individual images and Z-stacks. The Image J software (Wayne Rasband, National Institutes of Health, U.S.A.) was used to analyze F-actin levels (phalloidin staining), β-galactosidase and DE-Cadherin staining intensity, cell cross-sectional area and cell length. For all of these experiments we compared mutant cells with neighboring wild type cells. This was important as some cellular parameters vary as a function of position across the wing (e.g. cross sectional area). Statistical analysis of the data was done in Microsoft Excel (Microsoft) and/or Sigma Stat (SPSS).

In some of the experiments where we quantitatively analyzed confocal images we used the raw data and did not correct for background (e.g. non-specific staining, camera background). This approach underestimates the true change in staining when comparing mutant and wild type cells, but it was not always possible to get a “background” measurement that we were confident of (Waters, 2009; Wolf et al., 2007). In other experiments we made such corrections by subtracting from the signal the background staining as measured from a cellular region where we did not expect any signal (Waters, 2009). For example, in the β-galactosidase immunostaining measurements we used the staining intensity in the cytoplasm as a measure of background as in these experiments the β-galactosidase contained a nuclear localization signal (see Supplementary Fig. S1). When a correction was made for background it is noted in the text. A similar procedure was used to correct for background in experiments where we measured DE-cadherin levels. In this case we measured staining in the center of cells (not near the plasma membrane) to assess background. In general we did not correct for background when we compared levels of F-actin due to the difficulty in deciding how to measure background. The F-actin measurements were made on single optical sections from the level of the adherens junction. To measure central F-actin we drew a circle in the middle of the cell and measured mean F-actin levels. To measure peripheral F-actin we drew a line across the border between two mutant (or wild type cells) and measured the maximum fluorescence intensity.

Lat A test for F-actin depolymerization

The procedure followed has been described previously (Ren et al., 2007). Briefly, clone bearing pupal wings were dissected and incubated for various lengths of time at 25°C in Schneider's medium containing 50μM Latrunculin A (Sigma). The wings were then fixed and stained with Phalloidin and then images of clones obtained by confocal microscopy. The intensity of staining was quantified using Image J.

Results

Trc/Fry regulate cell shape differently than Wts/Mats

In wild type wing cells, hair initiation normally starts around 32 hours after white pupae formation (APF). Early studies on *trc* and *fry* described their strong multiple wing hair cell phenotypes (Cong et al., 2001; Geng et al., 2000) (Fig. 1A). Adult wing cells mutant for *wts* (Fig. 1B) or *mat*s (data not shown) typically showed a bulged apical surface and sometimes a multiple hair cell type (He et al., 2005a), albeit one that is weaker than *trc* or *fry* mutant phenotype. We previously noted that cells mutant for *trc*, *fry*, *wts* and *mats* showed two phenotypes prior to hair formation (He et al., 2005b). Cells mutant for any of these genes showed increased level of F-actin (Fig. 2A–F, S–X and data not shown), and the cross sectional area of *trc* and *fry* mutant cells was increased in contrast to the decreased cross sectional area of *wts* and *mats* mutant cells (Fig. 3).

Altered cross sectional area could reflect a change in cell volume and/or a change in cell shape. To distinguish between these possibilities, we obtained Z-stacks of clones by confocal microscopy. Reconstructions and Z projections were then derived. This allowed us to measure the height of mutant and neighboring wild type cells as well as cross sectional area. We found that *fry* (Fig. 2A–C, S–U, Fig. 3) and *trc* (Fig. 3 and data not shown) mutant cells had significantly larger cross sections, but there was no change in cell height. Thus, *trc* and *fry* mutations led to increased cell volume (Fig. 3). In contrast, *mats* (Fig. 2D–F, V–X) and *wts* (data not shown) mutant cells had significantly smaller cross sectional area but this was balanced by increased height so there was no difference in cell volume (Fig. 3).

Cells that lack Wts function are expected to have increased nuclear Yki and this is thought to be the cause of the *wts* tumor phenotype. We examined clones of cells that over-expressed Yki (generated by the flip out technique) (Huang et al., 2005). They shared the smaller cross sectional area and greater height of *wts* and *mats* mutant cells (Fig. 2G–I, Y-a). This suggested that the cell shape changes associated with *wts* and *mats* were mediated by alterations in the transcription of one or more Yki target genes in wing cells. As a complement to the *yki* over expression clones we also induced and examined both *yki* loss of function clones and *wts yki* double mutant clones. These failed to proliferate extensively, but we were able to recover small clones. These did not show an obvious change in cell shape (Fig. 2M–R). Similar observations Casual observations of *hippo* mutant clones suggested that they behaved similarly to *wts* and *mats* mutant cells although quantitative data was not obtained (Fig. S2).

Could the smaller cross section and greater height of the *wts* and *mats* mutant cells be a secondary consequence of their growing more rapidly than neighboring cells? To assess the relative growth of mutant and wild type cells we compared the number of cells in clones versus their neighboring twin spots. We found, as expected, that *wts* or *mats* mutant cells grew faster than the neighboring wild type cells (Fig. S3) and out-competed them. As a test of the hypothesis that the different relative growth rates were responsible for the changed cell shape, we examined the phenotype of Minute$^{+/-}$ mutant cells that were juxtaposed to clones of Minute$^{+/+}$ wild type cells. Minute cells grow more slowly than their wild type neighbors (Kongsuwan et al., 1985). Notably, we did not see any difference in cross sectional area or

height between Minute$^{+/-}$ and Minute$^{+/+}$ cells (Fig. 2J–L, b–d, Fig. 3). We also examined *trc* or *fry* mutant cells for effects on cell proliferation. We found those cells also grew more rapidly than their wild type twins (Fig. S3). However, in contrast to *wts* and *mats* clones *trc* and *fry* clones never came close to taking over an entire compartment. Perhaps the increased growth rate of *trc* and *fry* clones was transient or there was increased cell death in large clones. We concluded that the juxtaposition of cells with different cell division rates per se was unlikely to be the cause of the changes in cell shape/volume seen with *trc*, *fry*, *wts* or *mats* mutant cells.

trc, fry, wts and mats mutant cells all show increased levels of F-actin

In contrast to the opposite effects of *trc/fry* and *wts/mats* on cell shape, we found that cells mutant for each of these genes showed increased levels of F-actin (as assayed by Phalloidin staining, Fig. 2A–F, and data not shown). Compared to wild type cells significant increases were seen in the amount of F-actin at the cell periphery and in non-peripheral cytoplasm (Fig. 3). Once again we used *Minute*$^{+/-}$ cells as a control. We detected a small but significant increase in peripheral but not central F-actin levels between *Minute*$^{+/-}$ and wild type neighbors (Fig. 3). Thus, we concluded that relative growth rate could not explain the large differences seen in the levels of F-actin. We also observed increased F-actin in cells that over-expressed *yki* (Fig. 2G–I) and in clone cells that lacked *hpo* function (data not shown). We did not see any consistent change in F-actin in *yki* loss of function clones (Fig. 2M–O) or in *wts yki* double mutant cells (Fig. 2P–R).

The level of F-actin in cells is a result of the balance between polymerization and depolymerization. A mutation can result in increased F-actin due to increased filament stability (i.e. decreased rate of depolymerization) and/or increased polymerization of G-actin. An assay to distinguish between these two possibilities was developed in yeast (Okada et al., 2006). It was based on the ability of Latrunculin A (Lat-A) to block actin polymerization without affecting actin depolymerization. The rate at which F-actin disappeared in the presence of Lat-A was a measure of the relative rate of actin depolymerization and this could be compared for mutant and wild type cells. We previously adapted this assay for use in studying the effects of mutations on actin dynamics in pupal wing cells. This entailed incubating pupal wings that had marked clones in medium containing Lat-A for various lengths of time followed by fixation and staining with Phalloidin (Ren et al., 2007). Using this approach we found that the large increase in F-actin seen in cells mutant for *flare* (which encodes the fly AIP1) was due to an increase in F-actin stability. This made good sense as it is known from a variety of experiments that AIP1 interacts with cofilin to promote actin depolymerization (Ono, 2003). These experiments also showed the actin cytoskeleton was highly dynamic in pupal wing cells as F-actin levels fell more than 2 fold in wild type cells incubated for 18 minutes in Lat-A medium. We carried out this assay on wings bearing *wts* clones and found the rate of loss of F-actin staining was similar for both neighboring wild type and *wts* mutant cells (Fig. 4). This argued that the mutations did not alter F-actin depolymerization, and by elimination it suggested that the increased F-actin in the *wts* mutant cells was a consequence of increased actin polymerization. Attempts to carry out a similar experiment on *trc* were not successful as in vitro culture per se appeared to reduce the increased F-actin seen in mutant cells to close to wild type levels.

The distribution of tubulin is not dramatically changed in wts and fry clones

Fry has been found to bind to microtubules and to be required for the alignment of chromosomes on the mitotic spindle. We therefore examined the distribution of tubulin and acylated tubulin in wild type and *fry* and *wts* mutant pupal wing cells. We did not observe any change in tubulin or acylated tubulin prior to wing hair initiation (Fig. S4). The distribution in cells that contained growing hairs was affected to the extent that hair morphology was altered (data not shown).

DE-Cadherin was upregulated in trc, fr, wts and mats mutant cells

Relatively little is known about the mechanisms that regulate the height of epithelial cells, although there are suggestions that cell adhesion may play a role (Montell, 2008). Two types of experiments were done to determine if changes in cell adhesion could be responsible for the altered cell height and cross section seen in *wts* (and *mats*) and *trc* (and *fry*) mutant cells. In the first we examined the level of DE-Cadherin in *wts*, *mats*, *trc* and *fry* mutant cells. Interestingly DE-Cadherin levels increased in all of the four kinds of mutant cells (Fig. 5A–F and data not shown (*fry* and *mats*)). Since increased DE-Cadherin levels were observed in mutant cells that had opposite changes in cell shape, we concluded that the increased DE-Cadherin was unlikely to be the cause of the cell shape changes. We quantified DE-Cadherin levels for both *trc* and *wts* mutant clones and found the increases significant (Table 1A). After correcting for background staining (see Methods) we observed a 3.6 fold increase in *wts* mutant cells and a 2.5 fold increase in *trc* mutant cells. The greatest increase was seen at cell borders between two mutant cells with an intermediate value at borders between wild type and mutant cells (Fig. S5). This is reasonable, as one cannot distinguish by confocal microscopy between Cadherin molecules on neighboring cells. We also saw an increase in DE-Cadherin in cells that over-expressed Yki (Fig. 5G–I), suggesting that the increase seen in *wts* and *mats* mutant cells was likely due to the effect of increased nuclear Yki on the transcription of target genes. Most of the increased DE-Cadherin was still localized to adherens junctions in the mutant cells in these experiments so it seems likely to be functional (Fig. 5M–U). The increased level of DE-Cadherin could be due to many possible biochemical mechanisms (e.g. increased transcription, decreased turnover). The results with *yki* suggested that transcription was involved but such results could be due to a direct or indirect effect on *shg*, which encodes DE-cadherin in Drosophila. We used an enhancer trap insertion in the *shg* gene to look for effects on transcription. We observed a significant increase in lacZ immunostaining in both *wts* and *trc* mutant clone cells (compared to neighboring wild type cells) and in cells where *fry* expression was knocked down by expressing a *fry* ds-RNA from a transgene (Fig. 6, Table 1B). When corrected for background (see Methods) we observed increases that ranged from approximately 2.9 fold (*wts*) to 1.8 fold (*fry*) (Table 1B).

In the second set of experiments we examined cells where Gal4 was used to drive increased levels of DE-Cadherin. These cells were generated either by inducing flip out clones that expressed Gal4 or by using the *ptcGal4* driver combined with a temperature sensitive Gal80 that allowed us to restrict the time of over-expression. Both of these approaches lead to high levels of DE-Cadherin (Fig. 5J–L, 5V–X, and data not shown). However, we did not see increased cell height nor decreased cross section associated with the increased DE-Cadherin. Indeed, there was a hint of a possible decrease in cell height (Fig. 5V–X).

In other systems it has been observed that E-Cadherin can stimulate actin polymerization (Kovacs et al., 2002b). We saw a 1.3 fold increase in F-actin in cells that greatly over expressed DE-Cadherin (4 fold, as measured by immunostaining at the adherens junction) due to expression being driven by *ptcGal4* (Fig. 5J–L, 5V–X, and data not shown). The increased DE-Cadherin in *wts* and *trc* mutant cells likely contributed to the increased F-actin seen in these cells but it is unlikely to be the entire story. In both *wts* and *trc* clones we observed lesser increases in DE-Cadherin levels (3.6 and 2.5 fold respectively vs 4 fold with *ptc-GAL4* driven expression) but greater increases in F-actin level (1.9 and 1.4 fold respectively vs 1.3 fold). These data suggested that *wts* and *trc* targets other than DE-cadherin also contributed to the increased F-actin detected in mutant cells.

Wts/Mats and Trc/Fry alter the timing of hair morphogenesis in opposite directions

Wing hair initiation is delayed in *trc* or *fry* mutant cells, but precocious in *wts* and *mats* mutant cells (Fig. 7A–F and data not shown) (He et al., 2005b). We extended these observations and

found that cells over expressing Yki also showed precocious hair initiation (Fig. 7G–I). We also examined clones that were homozygous for a loss of function *yki* allele (yki^{B5}). These failed to proliferate extensively, however, we recovered small clones and these showed a delay in hair initiation (Fig. 7J–L). We examined cells that were doubly mutant for *wts* and *yki* and found these also showed a delay in hair initiation (Fig. 7S–U), hence *yki* is epistatic to *wts* for this phenotype. We concluded that the effects of *wts* and *mats* on the timing of hair morphogenesis were mediated by Yki and hence were likely due to effects on gene expression.

Again we used Minute wings as a control to determine if cell growth rate per se had an effect on the timing of differentiation. No difference was seen between $Minute^{+/-}$ cells and their wild type neighbors (Fig. 7M–O). Thus, we conclude that growth rate per se did not affect the timing of differentiation. At the later stages in hair morphogenesis, the effects of the different initiation time were greatly diminished. Results similar to this have been seen previously with different mutations (Ren et al., 2005) and are presumably due to the late initiating hairs “catching up”.

The change in the timing of hair initiation was consistent with the effects of the mutations on cell cross sectional area. To determine whether the change in cell shape/cross section area per se could be the cause of the change in the timing of wing hair initiation, we examined clones of polyploid cells homozygous for the *ultA* mutation (Adler, 2000). These cells had a substantially larger cross sectional area and a similar cell height compared to the wild type neighbors. No difference in the timing of hair initiation was seen in the *ultA* mutant clones (Fig. 7P–R), thus cross sectional area per se was not the cause of the changes in the timing of hair initiation.

Mwh and the timing of hair morphogenesis

The opposite phenotypes on the timing of wing hair initiation in *trc* (or *fry*) and *wts* (or *mats*) mutant clones suggested that the two gene modules might function in an antagonistic fashion to regulate the expression of downstream target genes. To test this possibility, we immunostained pupal wings to detect the endogenous Mwh protein in *trc, fry, wts* and *mats* mutant clones. The expression of *mwh* increases prior to hair formation and then the amount of Mwh remains relatively constant for more than 12 hours (Fig. S6) (Yan et al., 2008). We have found that it can be used as a reporter for the initiation of the hair morphogenesis gene expression program (Yan et al., 2008). In addition, the strong multiple hair cell phenotype of *mwh* is partly mimicked by the *trc* (or *fry*) mutant phenotype. We found decreased accumulation of Mwh in 31-hour APF *trc* (Fig. 8A–C) and *fry* (data not shown) mutant cells, and in contrast increased levels of Mwh in *wts* (Fig. 8D–F) and *mats* (data not shown) mutant cells. We considered two possible models to explain these observations. First, the changes could be due to a delay or advancement in the entire hair gene expression program. If the lowered accumulation of Mwh in the mutant clones was due to a delay in the entire hair gene expression program then at later stages in hair morphogenesis the levels of Mwh should be similar in wild type and mutant cells. Alternatively, it is possible that the mutations directly alter the expression of *mwh*, and in that case we expect that Mwh levels would still be changed at later stages.

To determine which hypothesis was correct, we immunostained both younger (25 hours APF) and older (35 hours APF) clone-bearing wings with anti-Mwh antibody. We found no obvious change in Mwh levels in the either early-stage (25APF) or late-stage (35APF) *wts*, *mats*, *trc* or *fry* mutant cells compared to their neighbors (Fig. S7), suggesting that the protein level change/accumulation of Mwh was due to the advancement (*wts* or *mats* mutations) or delay (*trc* or *fry* mutations) of the entire wing hair differentiation program.

To determine if the effect of Wts (or Mats) on Mwh was mediated through Yki we stained 30-hour APF pupal wings that contained marked UAS-*yki* over expressing cells. We saw increased Mwh immunostaining although this did not appear to be as strong as in *wts* or *mats* mutant

clones (Fig. 8G–I). The lesser effect could be due to *wts* or *mats* negative regulation of Yki, which was still functional in these cells. Once again the regulation was stage specific as no effect was seen in either 25-hour APF or 35-hour APF pupal wings (data not shown). Our data indicate that the regulation of Mwh by Wts or Mats was mediated through the Yki transcriptional factor, and the regulation of Mwh by Trc and Fry is in the opposite direction to that by Wts, Mats and Yki.

In a complementary set of experiments we asked if Mwh regulated Trc and Fry. We immunostained pupal wings that contained marked *mwh* clones, and found no change in either the level or the subcellular location of Trc or Fry (Fig. S8). This is consistent with Mwh functioning at the level of the cytoskeleton (Yan et al., 2008).

The observed decrease/delay in Mwh accumulation in *trc* or *fry* clones was unlikely to be the principal reason for the strong *trc* or *fry* multiple hair cell phenotype as *mwh trc* and *mwh fry* double mutants had a substantially stronger phenotype than either single mutant (Fig. 1G–I) (Cong et al., 2001). The double mutant phenotype was at least as strong as expected from the addition of the two single mutant phenotypes. These observations argued compellingly that *trc* or *fry* produced its strong multiple hair cell phenotype by functioning in parallel to *mwh*.

trc and wts function in parallel

Wing cells mutant for *trc* or *fry* displayed a very strong multiple hair cell phenotype, but the hairs were of relatively normal shape and polarity. The phenotype of *trc fry* double mutant cells was indistinguishable from either single mutant, consistent with these genes functioning in a common pathway (Cong et al., 2001). In contrast, *wts* and *mats* mutant cells showed apical bulging, retained pedestals and only occasionally formed multiple hairs. Such multiple hair cells were only seen in highly abnormal cells (He et al., 2005a). In adult flies, we found that some *yki* over expressing cells showed a multiple-hair phenotype, others the bulged tumor phenotype, and many cells showed both (Fig. 1D–F). Thus, *yki* over expressing cells displayed phenotypes typical of both *wts* and *trc* mutant cells (see Fig S9 for additional examples). This suggested the possibility that Trc, might like Wts, phosphorylate and negatively regulate Yki. As a test of this hypothesis we used enhancer trap insertions into the *diap1, CycE* and *ex* genes that are well-established readouts of Yki activity (Hamaratoglu et al., 2006; Huang et al., 2005). We did not see any alterations in the expression of these enhancer traps in *trc* mutant cells (Fig. S10), suggesting that Trc does not regulate Yki.

An alternative explanation for the *yki* over-expression multiple hair cell phenotype is that Yki might negatively regulate *trc* or *fry* expression. In this model *yki* over-expression would be equivalent to a hypomorphic *trc* (or *fry*) mutation. As a test of this possibility we immunostained *yki* over-expressing cells to detect the endogenous Trc and Fry proteins. In contrast to the expectations of the model we found increased levels of Trc and Fry immunostaining (Fig. S11). Thus, our data indicate that *yki* regulates the accumulation of Trc and Fry but this cannot explain the multiple-hair cell phenotype associated with *yki* over-expression.

As an additional test of whether Wts/Mats and Trc/Fry functioned in the same pathway in regulating hair formation and cell shape, we examined doubly mutant cells. We generated *wts trc* double mutant cells by inducing *wts* loss-of-function clones in wings where we over-expressed $trc^{S292A\ T453A}$ (a Trc dominant negative protein) (He et al., 2005a) in the *patched* (*ptc*) domain of the wing. The *wts* mutant clone outside the *ptc* domain served as control *wts* single mutant cells and non clone cells within the *ptc* domain served as control *trc* single mutant cells. The *wts* mutant clones inside the *ptc* domain were effectively *wts trc* double mutant cells. In *wts trc* double mutant cells, the phenotypes appeared to be additive (Fig. 1C). That is, the doubly mutant cells showed both the bulging cell phenotype (which is similar to the effect

caused by the single *wts* mutation, Fig. 1B) and the extreme multiple wing hair phenotype characteristic of *trc* mutation (Fig. 1A). The additivity of the double mutants argued that *trc* and *wts* function in parallel in wing cells.

Discussion

Connections between the Wts/Mats and the Trc/Fry pathways

The Hpo kinase is well known to function upstream of Wts. Recently, it was found that Hpo also functioned upstream of Trc in type IV da neurons (Emoto et al., 2006). In that study it was also shown that Hpo could be co-immunoprecipitated with both Trc and Wts and that Hpo could phosphorylate Trc at residue T453. This residue is conserved in homologs of Trc in other species, and its phosphorylation is essential for the kinase activity of Trc (Emoto et al., 2006; He et al., 2005b). In these cells Trc is required for dendrite tiling and Wts is required for the maintenance of dendrites (Emoto et al., 2006). *hpo* mutants showed defects in both dendrite tiling and maintenance, which is the additive phenotype of *trc* and *wts* mutations. We found in pupal wing cells that *hpo* mutants caused accelerated hair initiation and an increase in cell height. Both of these phenotypes mimic the phenotypes observed in *wts* or *mats* mutant cells. However, the increased cell length was not as dramatic as observed in *wts* or *mats* mutant cells, and we did not see a dramatic decrease in cell cross sectional area. That the *hpo* mutant phenotype was weaker than that of *wts* could be due to *hpo* regulating both *wts* and *trc* in the epidermis and these two targets having antagonistic phenotypes. However, we did not see evidence of a *trc*-like multiple hair cell phenotype in *hpo* mutant cells. Thus, it did not seem likely that *hpo* activity is essential for the activation of Trc in wing cells to insure that a single hair is formed.

The Yorkie transcription factor is the major downstream target of Hpo-Sav-Wts pathway. Phosphorylation of Yki by Wts leads to its movement from the nucleus to cytoplasm where it can no longer regulate gene expression (Dong et al., 2007; Zhang et al., 2008). Clones of cells that over-expressed Yki (due to a flip out *actin-Gal4* clone) sometimes showed a phenotype that could be interpreted as a result of the addition of individual *trc* and *wts* mutant phenotypes (Fig. 1). This raised the possibility that either Yki negatively regulated *trc* and *fry* or that Trc acted as a negative regulator of Yki. To test the former hypothesis, we immunostained *yki* over expressing cells to evaluate the level of Trc and Fry protein. In contrast to expectations of the model, Trc and Fry levels were increased. Thus, we cannot explain the multiple wing hair cell phenotype of *yki* over expression by it negatively regulating *trc* or *fry*. We suggest that multiple-hair cell phenotype associated with *yki* over expression is due to effects on the transcription of unidentified target genes involved in hair morphogenesis. In our experiments the over expression of *yki* resulted in a wider range of mutant phenotypes than *wts* loss of function clones. This could be due to the over expression by passing possible *wts* independent regulation of *yki* (Badouel et al., 2009)

An alternative hypothesis was that Trc negatively regulated Yki. The human Lats and Ndr proteins have the same substrate specificity (HXR/H/KXXS/T) *in vitro* (Hao et al., 2008; Zhao et al., 2007). A similar sequence surrounds Yki S168 (HSRARS^{168}), which is the site in Yki that is phosphorylated by Wts. Thus, it seemed possible that Trc, like Wts, might be able to phosphorylate and inactivate Yki. To test this hypothesis we asked if the expression of known transcriptional targets of Yki (*ex*, *diap1*, *CycE*) would be altered by a loss of *trc* activity. No effect on these targets was seen leading us to conclude that Trc did not regulate Yki. We suggest that differences in Trc and Wts that map outside of the conserved region (i.e. kinase domain) control this aspect of target specificity.

Actin, cell adhesion and cell shape are regulated by NDR kinases

F-actin levels in cells are a consequence of the balance between actin polymerization and depolymerization. Mutations in both *trc* and *wts* led to increased F-actin in wing cells. We used LatA to assess whether for *wts* this was due to effects on actin polymerization or depolymerization. These experiments showed the rate of actin depolymerization was similar in mutant clone cells and their wild type neighbors. Thus, we concluded that the difference in F-actin levels were due to *wts* resulting in increased actin polymerization. Other experiments argued that the effects of *wts* on F-actin levels were mediated through its regulation of Yki. This suggested that the action of *wts* was due to effects on gene expression and hence indirect and not due to Wts phosphorylating a protein directly involved in modulating actin polymerization.

Many factors are known to modulate actin polymerization during development. For example, in early embryos intercellular signaling plays a major role in regulating the location and density of cortical actin assembly. In particular, Cadherins have been implicated in regulating the actin cytoskeleton. In the early stages of epithelia formation F-actin assembles at the cytoplasmic domains of transmembrane Cadherins (Ehrlich et al., 2002; Jamora and Fuchs, 2002; Kovacs et al., 2002a; Kovacs et al., 2002b; Vaezi et al., 2002). In cultured cells, incubation with E-Cadherin can activate Rac1 and Cdc42, both of which are involved in actin polymerization and organization (Betson et al., 2002; Kim et al., 2000; Kovacs et al., 2002a; Nakagawa et al., 2001). A recent study showed that C-Cadherin expression is both necessary and sufficient for cortical actin assembly in *Xenopus* embryo (Tao et al., 2007). These observations combined with the increased level of DE-Cadherin seen in *trc*, *fry*, *wts* and *mats* mutant cells suggested the possibility that the increased cadherin could be the cause of the increased actin polymerization. However, we saw only a modest increase in F-actin levels in cells where we directed high levels of DE-Cadherin expression. Thus, while the increased DE-Cadherin in *trc* and *wts* mutant cells likely contributed to the increased level of F-actin it is likely that an alternative mechanism is also important.

There are several possible ways in which mutations in *trc*, *fry*, *wts*, and *mats* could lead to an increase in DE-Cadherin levels. Loss of *wts* or *mats* activity leads to an increase in nuclear Yki. If Yki acted as a positive regulator of DE-Cadherin expression this would provide a mechanism to increase DE-Cadherin levels. Consistent with this hypothesis we found that the expression of a *shg* enhancer trap was increased in *wts* mutant wing cells. Previous studies on *trc* and *fry* had not addressed their possible function in regulating transcription. In yeast is it well established that Cbk1p activates daughter cell gene expression in the bud by activating Ace2p (Nelson et al., 2003; Weiss et al., 2002). Cbk1p blocks the nuclear export of Ace2p by phosphorylation of the nuclear export signal. This leads to the daughter cell specific nuclear accumulation of Ace2p (Bourens et al., 2008). We found increased expression of the *shg* enhancer trap in *trc* clones and in cells where a *fry* ds-RNA was expressed. These results establish that these two genes regulate gene expression in flies and identify a target although the mechanism involved remains unknown.

In other systems it is known that DE-Cadherin accumulation is regulated by post-transcriptional mechanisms. In human MCF-cells, E-Cadherin level at the cell surface is actively regulated by both the endocytosis and the recycling of internalized E-Cadherin (Bryant et al., 2007). Both EGF signaling and Rac1-modulated macropinocytosis are thought to be involved (Bryant et al., 2007). Similar regulation of DE-Cadherin was also found in flies. The *Drosophila* EGF receptor homolog (EGFR) genetically interacts with DE-Cadherin, and EGFR could be co-immunoprecipitated with DE-Cadherin and Armadillo in the *Drosophila* embryo (Dumstrei et al., 2002). At this time we know of no evidence that *trc* or *wts* is involved in such processes but we cannot rule out the possibility that NDR family kinases regulate DE-Cadherin accumulation by multiple mechanisms.

An alternative hypothesis is that the increased DE-Cadherin immunostaining seen in *wts* or *mats* mutant cells was not due to increased cellular levels of the protein but rather to the smaller cross sectional area seen in these cells. If the same amount of DE-Cadherin was distributed over this shorter periphery the local concentration would be increased. Our experiments were not able to determine if other aspects of the adherens junctions were also changed (e.g. density, distance they occupy along the apical/basal axis). However, on the whole our data argue against this being the major mechanism involved. The relative increase measured in DE-Cadherin was substantially greater (~3.6) than the decrease seen in the cellular periphery (~1.2). Further, we observed an increase in expression of a *shg* enhancer trap in *wts* mutant cells and this cannot be explained by decreased cell periphery. Note that changes in cell periphery cannot explain the increased DE-Cadherin staining in *trc* mutant cells where cross section is increased. Indeed, we would expect a lower density of DE-Cadherin staining in *trc* or *fry* mutant cells if there was no overall change in DE-Cadherin levels.

Tissue shape and NDR kinases

The pupal wing is comprised of two simple epithelial sheets separated by a thin extra-cellular matrix. Except for the cells that form the veins the wing cells are all the same height and extend from the basement membrane to the common apical surface. We suggest the flat surfaces of the wing are a consequence of lattice of adherens junctions constraining the cells (Fig. 9). Interestingly, when we examined *wts* or *mats* clones the cells were typically taller than their neighbors. In small clones this was accommodated by the apical surface remaining flat and the basal surface being deformed. This deformation resulted in a shortening of the wild type cells juxtaposed across the basement membrane from the *wts* or *mats* mutant cells. This suggested that the *wts* or *mats* mutant cells are stiffer than normal wild type cells and as they lengthen they deform the juxtaposed cells. In larger *wts* or *mats* mutant clones the wing was often bulged (Fig. S12). We suspected that this was at least partially a consequence of the extra cell proliferation and the need to accommodate more cells on one surface than the other. The need to accommodate more cells on one wing surface than the other might also have played a role in the lengthening of *wts* or *mats* mutant cells in the smaller clones. The compression due to the crowding could provide the force that drives the increased cell height. It has previously been suggested that such compression could provide a growth control signal and this might be defective in *wts* or *mats* mutant cells (Aegerter-Wilmsen et al., 2007;Shraiman, 2005).

Hair differentiation program and NDR kinases

Oncogenic transformation and cancer are usually associated with defects in terminal differentiation (Alberts et al., 2002). Indeed, decreased differentiation, together with increased proliferation rate and reduced adhesion are often positively associated with more aggressive and invasive tumor behavior in cancer (Koivisto and Salaspuro, 1998). Wts and Mats are both tumor suppressors, thus it was quite surprising that cells that lacked function for these genes showed precocious hair differentiation and increased DE-Cadherin staining. This is opposite to what is normally associated with genetic changes that lead to tumors. Over expression of Yki also leads to both overgrowth and precocious terminal differentiation, thus both phenotypes are likely a consequence of altered gene expression. How can we explain a single genetic change being associated with this unusual set of phenotypes? We suggest that both phenotypes are due to context dependent changes in gene expression. The assortment and activity of other transcription factors in wing cells varies as a consequence of developmental stage (e.g. the stimulation of adult differentiation by ecdysone leads to a new set of active transcription factors) (Thummel, 1996). Enhancers in many genes would integrate the activities of Yki/Sd (or Yki interacting with an alternative partner) with other factors. In a cell with increased Yki activity prior to the hormonal stimulation for adult terminal differentiation the gene expression program would promote growth and inhibit apoptosis leading to the over growth phenotypes of *wts* or *mats* mutations. After the appropriate hormonal stimulation, Yki

activity would promote the expression of genes that are part of the terminal differentiation program leading to precocious differentiation.

Supplementary Material

Refer to Web version on PubMed Central for supplementary material.

Acknowledgments

This work was supported by grants from the NIGMS to pna. We thank Jeannette Charlton for help with some of the experiments. We thank the many members of the fly community for sending us reagents, particularly D.J. Pan, G. Halder and the Drosophila stock center at Indiana University.

References

Adler PN, Liu J, Charlton J. Cell size and the morphogenesis of wing hairs in Drosophila. Genesis 2000;28:82–91. [PubMed: 11064425]

Aegerter-Wilmsen T, Aegerter CM, Hafen E, Basler K. Model for the regulation of size in the wing imaginal disc of Drosophila. Mechanisms of Development 2007;124:318–326. [PubMed: 17293093]

Alberts, B.; Johnson, A.; Lewis, J.; Raff, M.; Roberts, K.; Walter, P. Molecular Biology of the Cell. 4. 2002.

Badouel C, Gardano L, Amin N, Garg A, Rosenfeld R, Le Bihan T, McNeill H. The FERM-Domain Protein Expanded Regulates Hippo Pathway Activity via Direct Interactions with the Transcriptional Activator Yorkie. Developmental Cell 2009;16:411–420. [PubMed: 19289086]

Betson M, Lozano E, Zhang J, Braga VMM. Rac Activation upon Cell-Cell Contact Formation Is Dependent on Signaling from the Epidermal Growth Factor Receptor. J Biol Chem 2002;277:36962–36969. [PubMed: 12147707]

Bidlingmaier S, Weiss EL, Seidel C, Drubin DG, Snyder M. The Cbk1p Pathway Is Important for Polarized Cell Growth and Cell Separation in Saccharomyces cerevisiae. Mol Cell Biol 2001;21:2449–2462. [PubMed: 11259593]

Bourens M, Racki W, Becam AM, Panozzo C, Boulon S, Bertrand E, Herbert C. Mutations in a small region of the exportin Crm1p disrupt the daughter cell-specific nuclear localization of the transcription factor Ace2p in *Saccharomyces cerevisiae*. Biology of the Cell 2008;100:343–354. [PubMed: 18076379]

Bryant DM, Kerr MC, Hammond LA, Joseph SR, Mostov KE, Teasdale RD, Stow JL. EGF induces macropinocytosis and SNX1-modulated recycling of E-cadherin. J Cell Sci 2007;120:1818–1828. [PubMed: 17502486]

Chiba S, Ikeda M, Katsunuma K, Ohashi K, Mizuno K. MST2- and Furry-Mediated Activation of NDR1 Kinase Is Critical for Precise Alignment of Mitotic Chromosomes. Current Biology 2009;19:675–681. [PubMed: 19327996]

Colman-Lerner A, Chin TE, Brent R. Yeast Cbk1 and Mob2 Activate Daughter-Specific Genetic Programs to Induce Asymmetric Cell Fates. Cell 2001;107:739–750. [PubMed: 11747810]

Cong J, Geng W, He B, Liu J, Charlton J, Adler PN. The furry gene of Drosophila is important for maintaining the integrity of cellular extensions during morphogenesis. Development 2001;128:2793–2802. [PubMed: 11526084]

Dong J, Feldmann G, Huang J, Wu S, Zhang N, Comerford SA, Gayyed M, Anders RA, Maitra A, Pan D. Elucidation of a Universal Size-Control Mechanism in Drosophila and Mammals. Cell 2007;130:1120–1133. [PubMed: 17889654]

Du LL, Novick P. Pag1p, a Novel Protein Associated with Protein Kinase Cbk1p, Is Required for Cell Morphogenesis and Proliferation in Saccharomyces cerevisiae. Mol Biol Cell 2002;13:503–514. [PubMed: 11854408]

Dumstrei K, Wang F, Shy D, Tepass U, Hartenstein V. Interaction between EGFR signaling and DE-cadherin during nervous system morphogenesis. Development 2002;129:3983–3994. [PubMed: 12163402]

Ehrlich JS, Hansen MDH, Nelson WJ. Spatio-Temporal Regulation of Rac1 Localization and Lamellipodia Dynamics during Epithelial Cell-Cell Adhesion. Developmental Cell 2002;3:259–270. [PubMed: 12194856]

Emoto K, He Y, Ye B, Grueber WB, Adler PN, Jan LY, Jan YN. Control of Dendritic Branching and Tiling by the Tricornered-Kinase/Furry Signaling Pathway in Drosophila Sensory Neurons. Cell 2004;119:245–256. [PubMed: 15479641]

Emoto K, Parrish JZ, Jan LY, Jan YN. The tumour suppressor Hippo acts with the NDR kinases in dendritic tiling and maintenance. Nature 2006;443:210–213. [PubMed: 16906135]

Gallegos ME, Bargmann CI. Mechanosensory Neurite Termination and Tiling Depend on SAX-2 and the SAX-1 Kinase. Neuron 2004;44:239–249. [PubMed: 15473964]

Geng W, He B, Wang M, Adler PN. The tricornered Gene, Which Is Required for the Integrity of Epidermal Cell Extensions, Encodes the Drosophila Nuclear DBF2-Related Kinase. Genetics 2000;156:1817–1828. [PubMed: 11102376]

Hamaratoglu F, Willecke M, Kango-Singh M, Nolo R, Hyun E, Tao C, Jafar-Nejad H, Halder G. The tumour-suppressor genes NF2/Merlin and Expanded act through Hippo signalling to regulate cell proliferation and apoptosis. Nat Cell Biol 2006;8:27–36. [PubMed: 16341207]

Hao Y, Chun A, Cheung K, Rashidi B, Yang X. Tumor Suppressor LATS1 Is a Negative Regulator of Oncogene YAP. J Biol Chem 2008;283:5496–5509. [PubMed: 18158288]

He Y, Emoto K, Fang X, Ren N, Tian X, Jan YN, Adler PN. Drosophila Mob Family Proteins Interact with the Related Tricornered (Trc) and Warts (Wts) Kinases. Mol Biol Cell 2005a;16:4139–4152. [PubMed: 15975907]

He Y, Fang X, Emoto K, Jan YN, Adler PN. The Tricornered Ser/Thr Protein Kinase Is Regulated by Phosphorylation and Interacts with Furry during Drosophila Wing Hair Development. Mol Biol Cell 2005b;16:689–700. [PubMed: 15591127]

Hergovich A, Lamla S, Nigg EA, Hemmings BA. Centrosome-Associated NDR Kinase Regulates Centrosome Duplication. Molecular Cell 2007;25:625–634. [PubMed: 17317633]

Huang J, Wu S, Barrera J, Matthews K, Pan D. The Hippo Signaling Pathway Coordinately Regulates Cell Proliferation and Apoptosis by Inactivating Yorkie, the Drosophila Homolog of YAP. Cell 2005;122:421–434. [PubMed: 16096061]

Jamora C, Fuchs E. Intercellular adhesion, signalling and the cytoskeleton. Nat Cell Biol 2002;4:E101–E108. [PubMed: 11944044]

Justice RW, Zilian O, Woods DF, Noll M, Bryant PJ. The Drosophila tumor suppressor gene warts encodes a homolog of human myotonic dystrophy kinase and is required for the control of cell shape and proliferation. Genes Dev 1995;9:534–546. [PubMed: 7698644]

Kim SH, Li Z, Sacks DB. E-cadherin-mediated Cell-Cell Attachment Activates Cdc42. J Biol Chem 2000;275:36999–37005. [PubMed: 10950951]

Koivisto T, Salaspuro M. Acetaldehyde alters proliferation, differentiation and adhesion properties of human colon adenocarcinoma cell line Caco-2. Carcinogenesis 1998;19:2031–2036. [PubMed: 9855020]

Kongsuwan K, Yu Q, Vincent A, Frisardi MC, Rosbash M, Lengyel JA, Merriam J. A Drosophila Minute gene encodes a ribosomal protein. Nature 1985;317:555–558. [PubMed: 4047173]

Kovacs EM, Ali RG, McCormack AJ, Yap AS. E-cadherin Homophilic Ligation Directly Signals through Rac and Phosphatidylinositol 3-Kinase to Regulate Adhesive Contacts. J Biol Chem 2002a; 277:6708–6718. [PubMed: 11744701]

Kovacs EM, Goodwin M, Ali RG, Paterson AD, Yap AS. Cadherin-Directed Actin Assembly: E-Cadherin Physically Associates with the Arp2/3 Complex to Direct Actin Assembly in Nascent Adhesive Contacts. Current Biology 2002b;12:379–382. [PubMed: 11882288]

Lai ZC, Wei X, Shimizu T, Ramos E, Rohrbaugh M, Nikolaidis N, Ho LL, Li Y. Control of Cell Proliferation and Apoptosis by Mob as Tumor Suppressor, Mats. Cell 2005;120:675–685. [PubMed: 15766530]

Luca FC, Winey M. MOB1, an Essential Yeast Gene Required for Completion of Mitosis and Maintenance of Ploidy. Mol Biol Cell 1998;9:29–46. [PubMed: 9436989]

Maki C, Rhoads D, Stewart M, Van Slyke B, Roufa D. The Drosophila melanogaster RPS17 gene encoding ribosomal protein S17. Gene 1989;79:289–298. [PubMed: 2507396]

Marygold SJ, Roote J, Reuter G, Lambertsson A, Ashburner M, Millburn GH, Harrison PM, Yu Z, Kenmochi N, Kaufman TC, Leevers SJ, Cook KR. The ribosomal protein genes and Minute loci of Drosophila melanogaster. Genome Biol 2007;8:R216. [PubMed: 17927810]

Mikeladze-Dvali T, Wernet MF, Pistillo D, Mazzoni EO, Teleman AA, Chen YW, Cohen S, Desplan C. The Growth Regulators warts/lats and melted Interact in a Bistable Loop to Specify Opposite Fates in Drosophila R8 Photoreceptors. Cell 2005;122:775–787. [PubMed: 16143107]

Montell DJ. Morphogenetic Cell Movements: Diversity from Modular Mechanical Properties. Science 2008;322:1502–1505. [PubMed: 19056976]

Nakagawa M, Fukata M, Yamaga M, Itoh N, Kaibuchi K. Recruitment and activation of Rac1 by the formation of E-cadherin-mediated cell-cell adhesion sites. J Cell Sci 2001;114:1829–1838. [PubMed: 11329369]

Nelson B, Kurischko C, Horecka J, Mody M, Nair P, Pratt L, Zougman A, McBroom LDB, Hughes TR, Boone C, Luca FC. RAM: A Conserved Signaling Network That Regulates Ace2p Transcriptional Activity and Polarized Morphogenesis. Mol Biol Cell 2003;14:3782–3803. [PubMed: 12972564]

Okada K, Ravi H, Smith EM, Goode BL. Aip1 and Cofilin Promote Rapid Turnover of Yeast Actin Patches and Cables: A Coordinated Mechanism for Severing and Capping Filaments. Mol Biol Cell 2006;17:2855–2868. [PubMed: 16611742]

Ono S. Regulation of Actin Filament Dynamics by Actin Depolymerizing Factor/Cofilin and Actin-Interacting Protein 1: New Blades for Twisted Filaments. Biochemistry 2003;42:13363–13370. [PubMed: 14621980]

Racki WJ, Bécam AM, Nasr F, Herbert CJ. Cbk1p, a protein similar to the human myotonic dystrophy kinase, is essential for normal morphogenesis in Saccharomyces cerevisiae. The EMBO Journal 2000;19:4524–4532. [PubMed: 10970846]

Ren N, Charlton J, Adler PN. The flare Gene, Which Encodes the AIP1 Protein of Drosophila, Functions to Regulate F-Actin Disassembly in Pupal Epidermal Cells. Genetics 2007;176:2223–2234. [PubMed: 17565945]

Ren N, Zhu C, Lee H, Adler PN. Gene Expression During Drosophila Wing Morphogenesis and Differentiation. Genetics 2005;171:625–638. [PubMed: 15998724]

Shraiman BI. Mechanical feedback as a possible regulator of tissue growth. Proceedings of the National Academy of Sciences of the United States of America 2005;102:3318–3323. [PubMed: 15728365]

Tao Q, Nandadasa S, McCrea PD, Heasman J, Wylie C. G-protein-coupled signals control cortical actin assembly by controlling cadherin expression in the early Xenopus embryo. Development 2007;134:2651–2661. [PubMed: 17567666]

Thummel C. Files on steroids--Drosophila metamorphosis and the mechanisms of steroid hormone action. Trends Genet 1996;12:306–10. [PubMed: 8783940]

Vaezi A, Bauer C, Vasioukhin V, Fuchs E. Actin Cable Dynamics and Rho/Rock Orchestrate a Polarized Cytoskeletal Architecture in the Early Steps of Assembling a Stratified Epithelium. Developmental Cell 2002;3:367–381. [PubMed: 12361600]

Verde F, Wiley DJ, Nurse P. Fission yeast orb6, a ser/thr protein kinase related to mammalian rho kinase and myotonic dystrophy kinase, is required for maintenance of cell polarity and coordinates cell morphogenesis with the cell cycle. Proceedings of the National Academy of Sciences of the United States of America 1998;95:7526–7531. [PubMed: 9636183]

Racki, Waldemar J.; AMB; Nasr, Fahd; Herbert, Christopher J. Cbk1p, a protein similar to the human myotonic dystrophy kinase, is essential for normal morphogenesis in Saccharomyces cerevisiae. The EMBO Journal 2000;19:4524–4532. [PubMed: 10970846]

Waters JC. Accuracy and precision in quantitative fluorescence microscopy. J Cell Biol 2009;185:1135–1148. [PubMed: 19564400]

Wei X, Shimizu T, Lai ZC. Mob as tumor suppressor is activated by Hippo kinase for growth inhibition in Drosophila. The EMBO Journal 2007;26:1772–1781. [PubMed: 17347649]

Weiss EL, Kurischko C, Zhang C, Shokat K, Drubin DG, Luca FC. The Saccharomyces cerevisiae Mob2p-Cbk1p kinase complex promotes polarized growth and acts with the mitotic exit network to facilitate daughter cell-specific localization of Ace2p transcription factor. J Cell Biol 2002;158:885–900. [PubMed: 12196508]

Wolf, DE.; Samarasekera, C.; Swedlow, JR.; Greenfield, S.; David, EW. Methods in Cell Biology. Vol. 81. Academic Press; 2007. Quantitative Analysis of Digital Microscope Images; p. 365-396.

Wu S, Liu Y, Zheng Y, Dong J, Pan D. The TEAD/TEF Family Protein Scalloped Mediates transcriptional Output of the Hippo Growth-Regulatory Pathway. Developmental Cell 2008;14:388–398. [PubMed: 18258486]

Yan J, Huen D, Morely T, Johnson G, Gubb D, Roote J, Adler PN. The multiple-wing-hairs Gene Encodes a Novel GBD-FH3 Domain-Containing Protein That Functions Both Prior to and After Wing Hair Initiation. Genetics 2008;180:219–228. [PubMed: 18723886]

Zallen JA, Peckol EL, Tobin DM, Bargmann CI. Neuronal Cell Shape and Neurite Initiation Are Regulated by the Ndr Kinase SAX-1, a Member of the Orb6/COT-1/Warts Serine/Threonine Kinase Family. Mol Biol Cell 2000;11:3177–3190. [PubMed: 10982409]

Zhang L, Ren F, Zhang Q, Chen Y, Wang B, Jiang J. The TEAD/TEF Family of Transcription Factor Scalloped Mediates Hippo Signaling in Organ Size Control. Developmental Cell 2008;14:377–387. [PubMed: 18258485]

Zhao B, Wei X, Li W, Udan RS, Yang Q, Kim J, Xie J, Ikenoue T, Yu J, Li L, Zheng P, Ye K, Chinnaiyan A, Halder G, Lai ZC, Guan KL. Inactivation of YAP oncoprotein by the Hippo pathway is involved in cell contact inhibition and tissue growth control. Genes & Development 2007;21:2747–2761. [PubMed: 17974916]

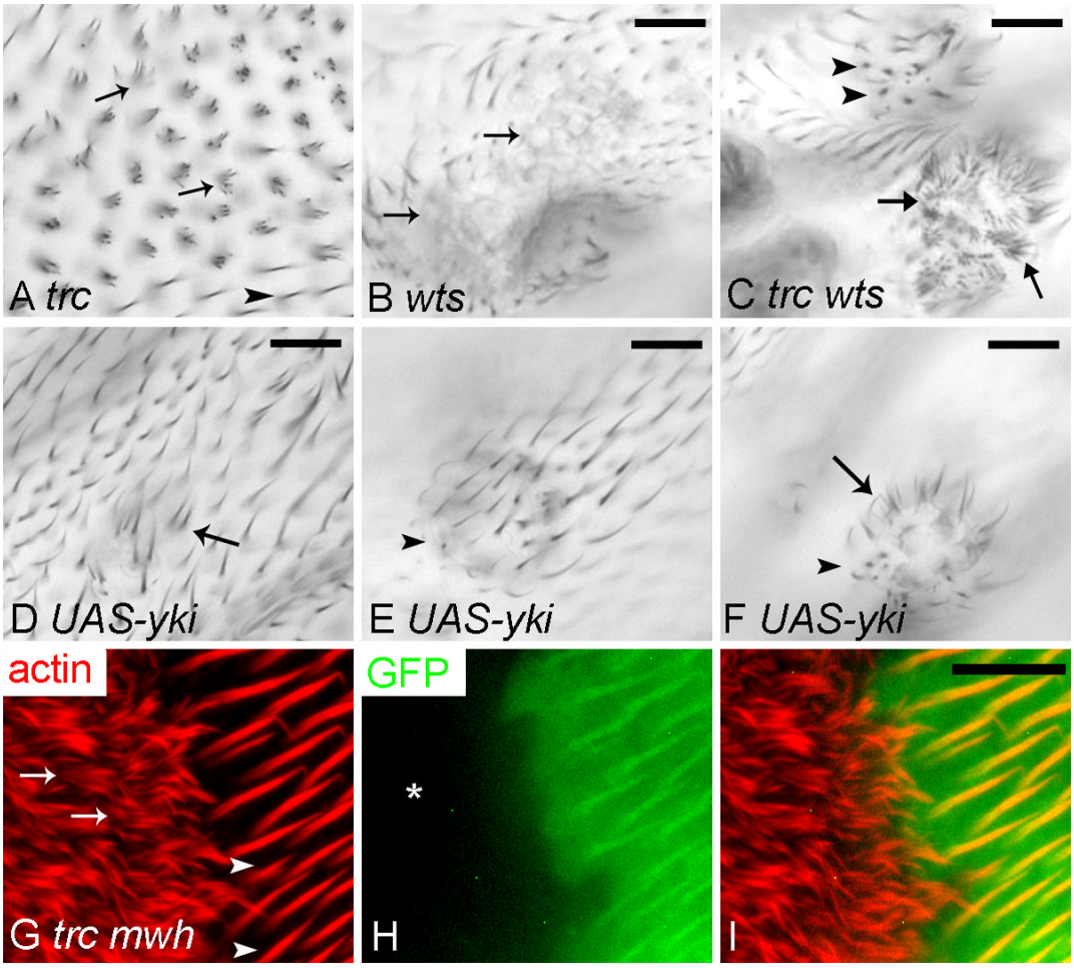

Fig. 1.

Wing hair phenotypes of *trc*, *wts*, *UAS-yki* over expression, *wts trc* double mutant and *mwh trc* double mutant cells. Panel A showed a trc^{1} clone in an adult wing. Notice the strong multiple hair cell phenotype (arrow points to multiple hairs, arrow head points to wild type hair). Panel B showed a small wts^{P3} clone in an adult wing. Notice the outlines of bulged cells (arrow). Panel C showed a small group of $trc^{S292A\ T453A}$ wts^{P3} double mutant cells (genotype: *w hs-flp; UAS-*$trc^{S292A\ T453A}$*/ptc-Gal4 UAS-MCD8-GFP; FRT 82* wts^{P3}*/FRT82 tub-gal80*). Note the bulged out region and the extreme multiple hair cell phenotype (arrow) inside *patched* domain. *wts* single mutant clones outside the *ptc* domain showed the *wts* bulged cell/tumor phenotype (arrowheads). Panels D–F showed three *actinGal4 UAS-yki* flip out clones. Panel D showed the multiple hair cell phenotype of a small clone which was induced in the pupal stage. Arrow points to multiple hair cells. Panel E showed a clone, which was induced earlier that contained bulged cells (arrowhead) but no multiple-hair cells. Panel F showed a clone that displays both bulging (arrowhead) and a strong multiple hair cell phenotype (arrow). Panels G–I showed a *mwh* trc^{1} double mutant clone in a pupal wing marked by the loss of GFP. The pupal wing is also stained with Alexa 568 phalloidin to showed hairs (in red). Panel G showed F-actin alone, panel H GFP alone and panel I the merge. Arrows point to cells with extreme multiple hair cell phenotype, and arrowheads to single hairs of wild type cells. The asterisk marks the clone region that lacks GFP. Scale bar is 10 μm.

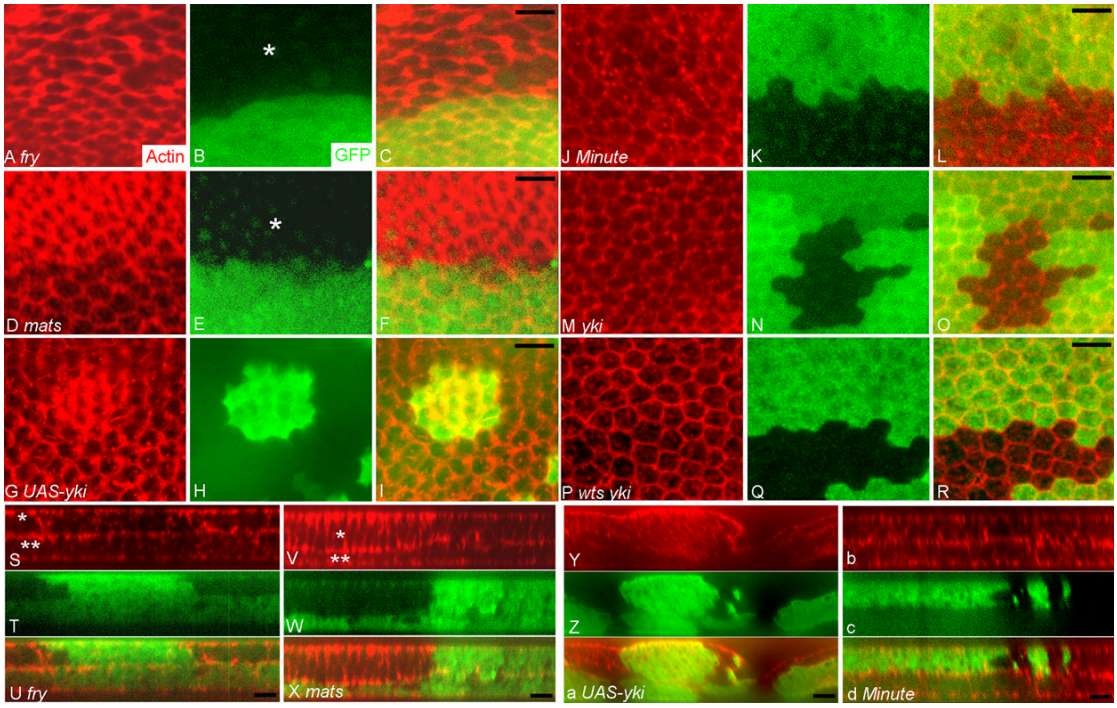

Fig. 2.

trc, *fry*, *wts*, *mats* and *yki* regulate cell shape and intracellular F-actin level. Panels showed clones marked by the loss or gain of GFP (green) and stained with phalloidin (red) to showed the distribution of F-actin. In each case, red, green and merged images are shown. Panels A–C showed a fry^{T2K61} clone (marked by an asterisk). Note the mutant cells have increased F-actin and larger cross section comparing to wild type neighbors (as judged by peripheral F-actin staining). Panels D–F showed a $mats^{e03077}$ clone (asterisk). Note the clone cells have a smaller cross section comparing to wild type cells and stain more intensely for F-actin. Panels G–I showed a Gal4 flip out clone that over-expressed Yki from a *UAS-yki* transgene. The clone is marked by the expression of GFP. Note the GFP expressing cells have a smaller cross section and increased F-actin. Panels J–L showed a $Minute^{+/-}$ clone marked by the expression of GFP surrounded by $Minute^{+/+}$ cells that don't express GFP. Panels M–O showed a yki^{B5} clone (marked by loss of GFP). Panels P–R showed a wts^{P3} yki^{B5} double mutant clone (marked by loss of GFP). Panels S–U showed Z axis reconstructions through a fry^{T2K61} clone (marked by loss of GFP). There is bright F-actin staining at the apical (asterisk) and basal (double asterisks) levels of the mutant cells. The wing is composed of two simple epithelial cell layers with their basal surfaces juxtaposed. Panels V–X showed the Z axis reconstruction through a $mats^{e03077}$ clone. Note the clone cells on the distal surface are taller (asterisk) and this results in the compression and shortening of the juxtaposed ventral non-clone cells (double asterisks). Note also the increased F-actin staining in the clone cells. Panels Y-a showed a Z axis reconstruction a *UAS-yki* flip out clone. Note the clone cells are taller. Panels b–d showed a $Minute^{+/-}$ clone. Note there is no change in cell height. Scale bar in all panels is 10 μm.

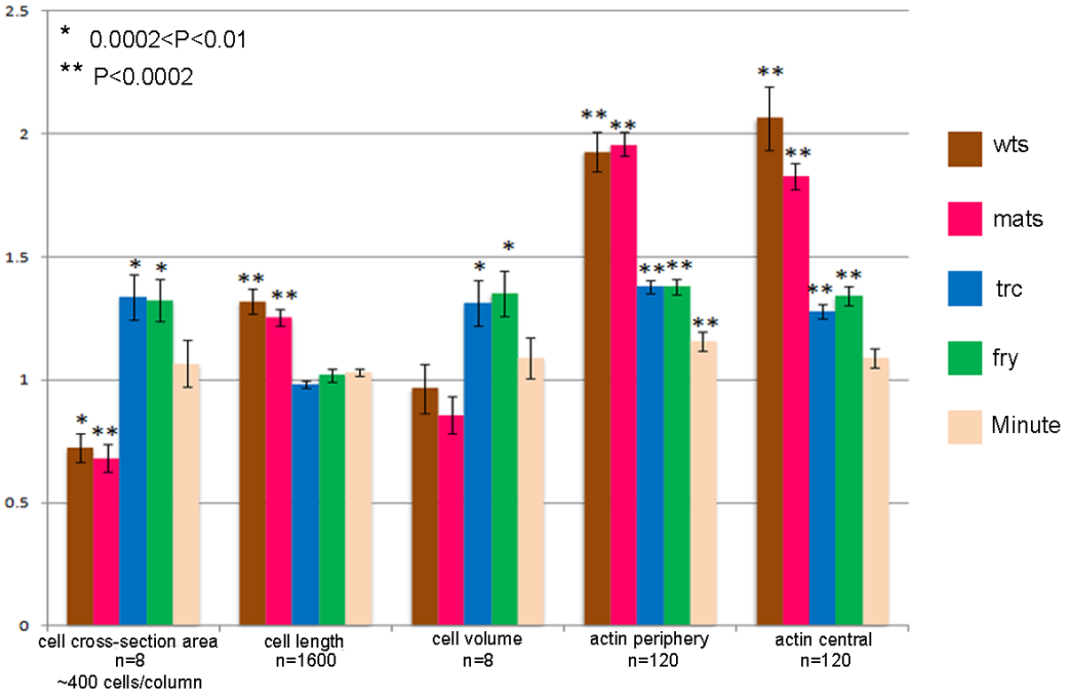

Fig. 3.

Summary of the cell shape and F-actin level analysis of *trc*, *fry*, *wts*, *mats* and *Minute* mutant cells. Bars showed the mean ratios for the 5 measured parameters. The ratios were obtained from measurement of mutant to neighboring wild type cells. Error bars showed the standard error of the mean. Samples where the mutant and wild type means were significant with a $p<0.01$ are identified by an asterisk, samples where the $p<0.0002$ are identified with double asterisks. T-tests were used to compare the values from mutant and wild type cells. Data for each column were collected from eight individual wings. Cell cross-section area, ~400 cells observed/column (n=8) cell length, 3200 cells observed/column (half wild type and half mutant, n=1600); cell volume, 16 clones analyzed (by multiplying average cell cross-section area by average cell height in each clone)/colum (n=8); actin periphery, 240 cells observed/column (n=120); actin central 240 cells observed/column (n=120).

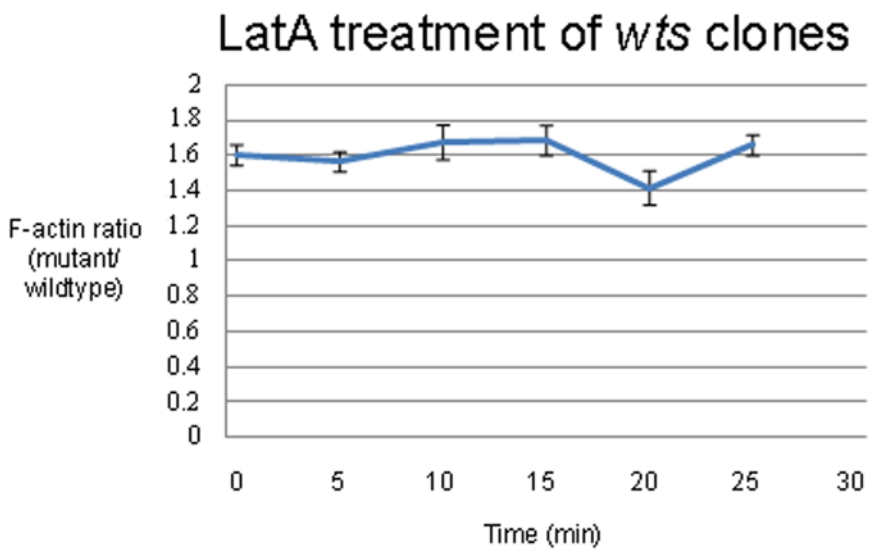

Fig. 4.

Ratio of F-actin staining as a function of time of incubation in LatA.

The ratio of F-actin staining of *wts*^{P3} mutant clones to neighboring wild type cells as a function of time of incubation in Lat A. The error bars showed the standard error of the mean. The T-test P value of mutant-wild type cell comparison is <0.005 for all time points.

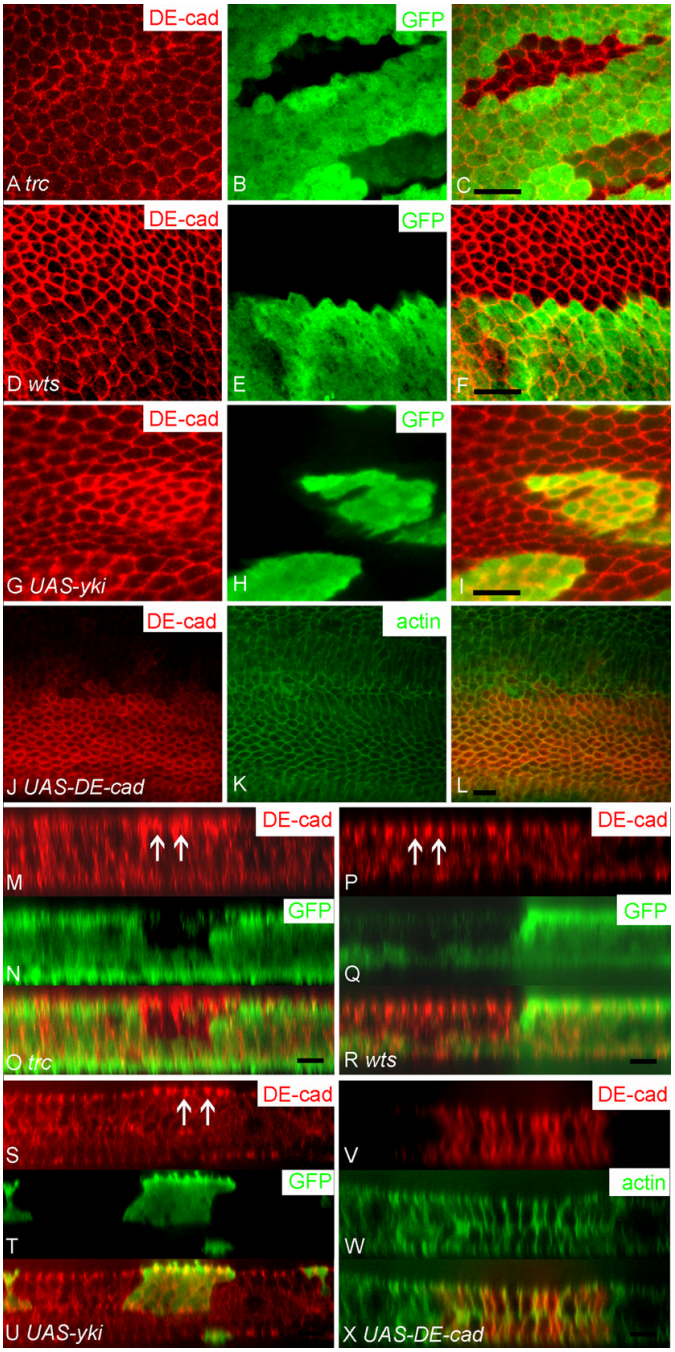

Fig. 5.

DE-Cadherin level was up-regulated in *trc*, *fry*, *wts* and *mats* mutant cells. For most panels DE-Cadherin immunostaining is shown in red and GFP, which was used to mark clones, is shown in green. A merged image is also shown. Panels A–C showed a trc^{P} clone marked by the loss of GFP. Note the increased DE-Cadherin immunostaining of clone cells. Panels D–F showed a wts^{P3} clone marked by the loss of GFP. Note the smaller cross section and increased DE-Cadherin staining of the mutant cells. Panels G–I showed a flip out clone marked by GFP expression that over expressed Yki. Note the increased DE-Cadherin staining of the clone cells. Panels J–L showed wings that over expressed DE-Cadherin in the *patched* domain. In these panels DE-Cadherin staining is shown in red and phalloidin staining in green. Note there is a

slight increase in F-actin in the *ptc* domain cells. Panels M–X are Z axis reconstructions of clones similar to those shown in panels A–L. Clones are shown for trc^{P} (in panels M–O) and wts^{P3} (panels P–R), which both showed increased DE-Cadherin staining (arrows). Panels S–U showed a Z axis reconstruction through a flip out clone that over expressed Yki. Note the increased DE-Cadherin staining (arrows). Panels V–X showed a reconstruction through a *patched* domain where DE-Cadherin is over expressed (red). Note that there is a slight decrease of cell height in the *patched* domain (middle part). Scale bar is 10 μm.

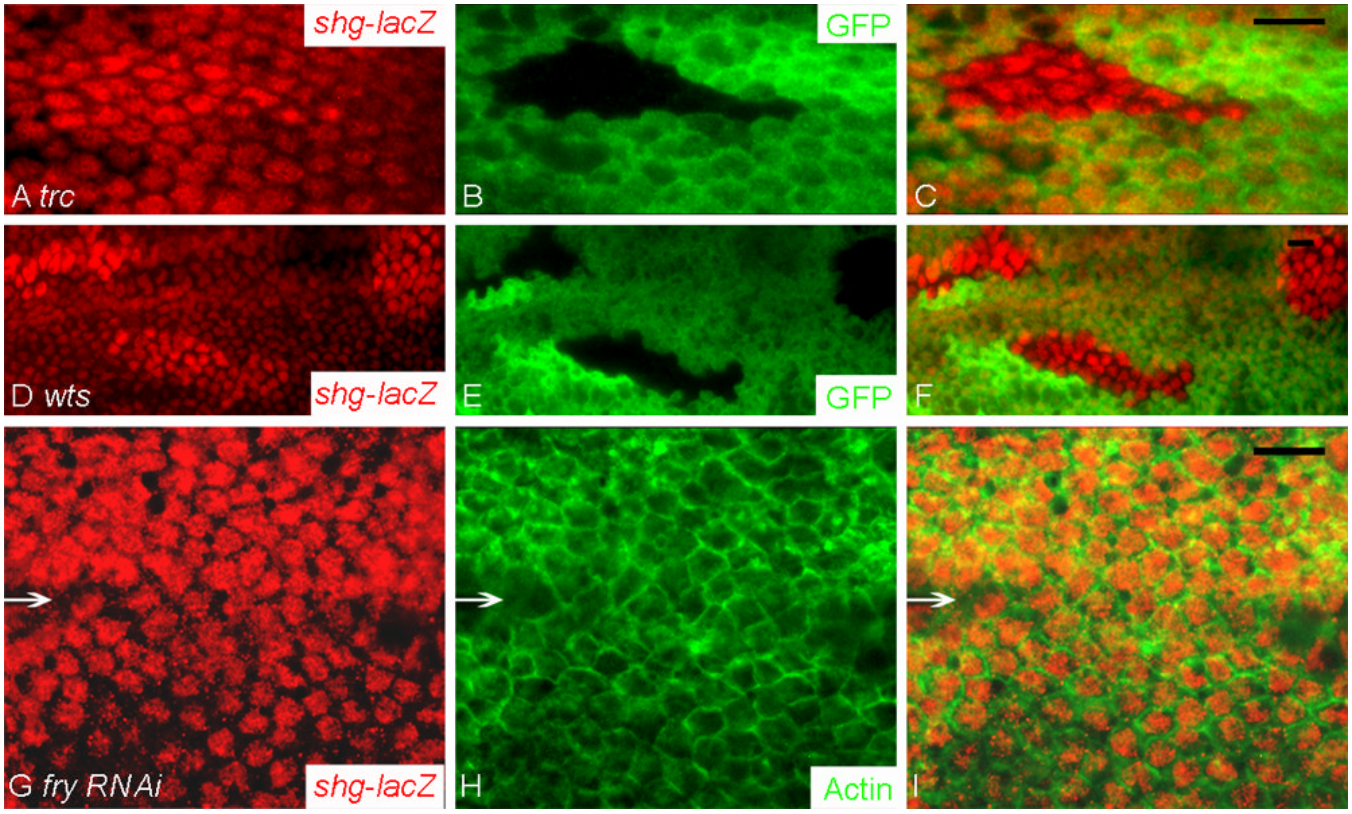

Fig. 6.

shg expression was up regulated in *wts* and *trc* (and *fry*) mutant cells. *shg* transcription was assayed using the lacZ enhancer trap as a reporter.

Panels A–C showed a trc^{P} clone marked by the loss of GFP. Panel A showed the lacZ staining (red). Panel B showed the GFP staining (green). Panel C showed the merged picture. Panels D–F showed three wts^{P3} clones marked by the loss of GFP. Panel D showed the lacZ staining (red). Panel E showed the GFP staining (green). Panel F showed the merged picture. Panels G–I showed cells where *fry* level was knocked down by expressing fry dsRNA. Arrows point to the border demarcating the patched domain. The upper part is inside the patched domain where the dsRNA was expressed using the *ptc-Gal4* driver. The lower part is outside the patched domain where the cells are wild type. Panel G showed the lacZ staining (red). Panel H showed the F-actin staining (green). Panel I showed the merged picture. Scale bar is 10μm.

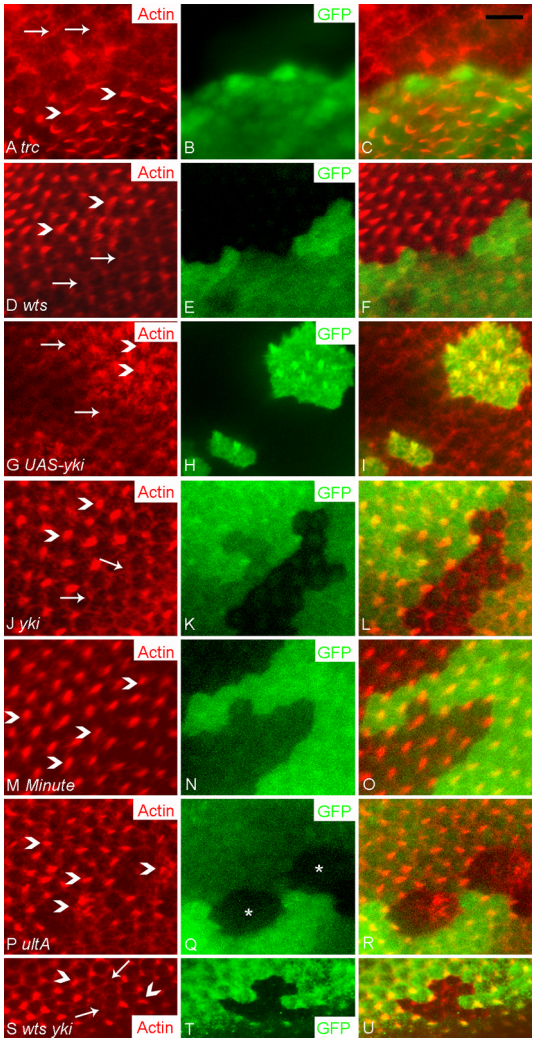

Fig. 7.

trc, *fry*, *wts* and *mats* regulate the time for pupal wing hair initiation. Clones are marked either by the loss (trc, wts, yki, ultA and wts yki double mutants) or gain (for *UAS-yki* flip out clones and Minute clones) of GFP expression (green). F-actin staining (red) is used to assess whether or not hairs have begun to form. A merged image is also shown. Panels A–C showed a trc^{P} clone. Note the larger cross section and delay in hair initiation comparing to neighboring wild type cells (in these and other panels arrows point to cells that haven't formed hairs, arrowheads to cells formed hairs). Panels D–F showed a wts^{P3} clone. Panels G–I showed a *UAS-yki* flip out clone. Panels J–L showed a yki^{B5} mutant clone. Note the lack of hairs at a time when neighbors showed hairs. Panels M–O showed a Minute $^{+/-}$ clone and Panels P–R *ultA* clones. Note the large *ultA* cells (asterisks and lack of GFP) do not appear to have an altered time of hair initiation. As seen previously the large *ultA* clone cells form multiple hairs (Adler, 2000). Panels S–U showed a wts^{P3} yki^{B5} double mutant clone (marked by loss of GFP) that displays delayed hair formation. . Scale bar is 10 μm.

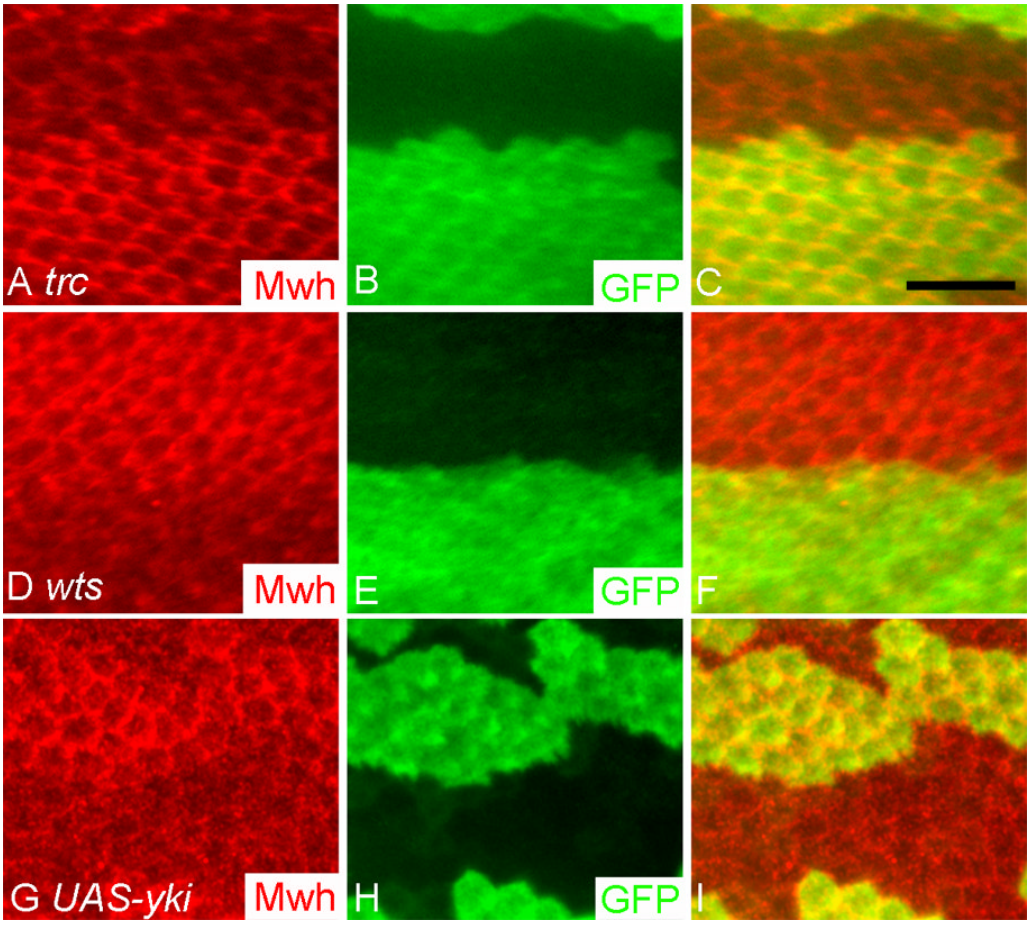

Fig. 8.

Mwh expression is regulated by *trc*, *fry*, *wts*, *mats* and *yki*.

In all panels, clones are marked by the loss (trc and wts clones) or gain (*UAS-yki* flip out clones) of GFP (green). Mwh immunostaining is shown in red and a merged image is also shown. Panels A–C showed a trc^{P} clone and panels D–F a wts^{P3} clone. Note the decrease in Mwh staining in the trc^{P} clone and the increase in Mwh staining in the wts^{P3} clone. Panels G–I showed a *UAS-yki* flip out clone. Note the increase in Mwh accumulation in the cells that overexpressed Yki. Scale bar is 10 μm.

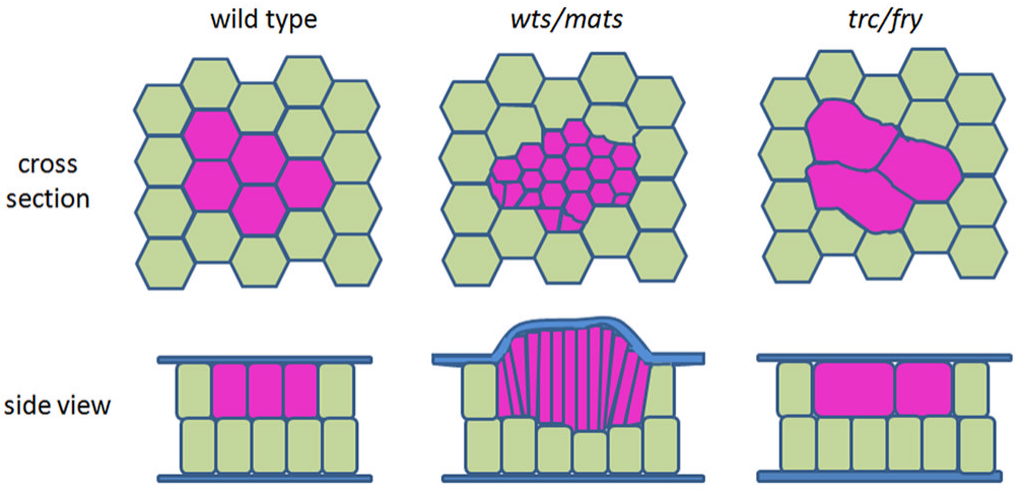

Fig. 9.

A cartoon model showing the changes of cross section area and cell height in the *wts* (or *mats*) or *trc* (or *fry*) mutant cells (purple) comparing to wild type cells (olive green). Minute$^{+/-}$ cells don't showed a cell shape change and fit in the wild type cell model. The blue outline in the cross section view represents a lattice of adherens junctions.

Dev Biol. Author manuscript; available in PMC 2011 May 15.

Table 1

A. *wts* and *trc* regulate DE-Cadherin level in wing cells.						
gene	**Type of treatment**	**Ratio – raw***	**Ratio – corrected#**	**Clone different*** Raw**	**Clone different corrected**	**n**
wts	clone	1.42(0.05**)	3.59(0.29**)	p<0.001	p<0.001	30
trc	clone	1.20(0.04)	2.50(0.30)	p<0.001	p<0.001	30
B. *wts*, *trc* and *fry* regulate *shg* expression in wing cells.						
Gene	Type of treatment	Ratio – raw*	Ratio – corrected#	Clone different* Raw	Clone different corrected	n
wts	clone	1.32 (0.012**)	2.86 (0.089)	p<0.001	p<0.001	96
fry	RNAi	1.29 (0.013)	1.78 (0.037)	p<0.001	p<0.001	60
trc	clone	1.19 (0.013)	1.95 (0.095)	p<0.001	p<0.001	26

* ratio = the maximum intensity of DE-Cadherin (in A) or lacZ (in B) immunostaining of cell periphery inside of the mutant clone (mutant-mutant cell border) divided by the value for that inside neighboring wild type cells (wild type-wild type cell border). Raw data was used with no correction.

the measured intensity values were corrected for background as described in the methods.

** the value in parentheses is the standard error.

*** a T test was used to compare intensities of wild type and mutant cells.